

Phonon-mediated superconductivity in orthorhombic *X*S (*X* = Nb, Ta or W)

Guo-Hua Liu(刘国华), Kai-Yue Jiang(江恺悦), Yi Wan(万一), Shu-Xiang Qiao(乔树祥), Jin-Han Tan(谭锦函), Na Jiao(焦娜), Ping Zhang(张平), and Hong-Yan Lu(路洪艳)

Citation: Chin. Phys. B, 2025, 34 (**2**): 027401. DOI: 10.1088/1674-1056/ad9733
Journal homepage: http://cpb.iphy.ac.cn; http://iopscience.iop.org/cpb

What follows is a list of articles you may be interested in

Prediction of novel layered indium halide superconductors

Zhi-Hong Yuan(袁志红), Jing-Jing Meng(孟静静), Rui Liu(刘瑞), Peng-Yu Zheng(郑鹏宇), and Zhi-Ping Yin(殷志平)

Chin. Phys. B, 2024, 33 (**10**): 107401. DOI: 10.1088/1674-1056/ad6a09

Experimental observation of Fermi-level flat band in novel kagome metal $CeNi_5$

Xue-Zhi Chen(陈学智), Le Wang(王乐), Shuai Zhang(张帅), Ren-Jie Zhang(张任杰), Yi-Wei Cheng(程以伟), Yu-Dong Hu(胡裕栋), Cheng-Nuo Meng(孟承诺), Zheng-Tai Liu(刘正太), Bai-Qing Lv(吕佰晴), and Yao-Bo Huang(黄耀波)

Chin. Phys. B, 2024, 33 (**8**): 087402. DOI: 10.1088/1674-1056/ad4019

Moiré superlattices arising from growth induced by screw dislocations in layered materials

Fuyu Tian(田伏钰), Muhammad Faizan, Xin He(贺欣), Yuanhui Sun(孙远慧), and Lijun Zhang(张立军)

Chin. Phys. B, 2024, 33 (**7**): 077403. DOI: 10.1088/1674-1056/ad4cdc

First-principles study of moderate phonon-mediated pairing in high-pressure monoclinic phase of BiS_2-based superconductors

Jie Cheng(程杰), Yu-Lan Cheng(程玉兰), Bin Li(李斌), and Sheng-Li Liu(刘胜利)

Chin. Phys. B, 2023, 32 (**10**): 107401. DOI: 10.1088/1674-1056/accd56

A ten-fold coordinated high-pressure structure in hafnium dihydrogen with increasing superconducting transition temperature induced by enhancive pressure

Yan-Qi Wang(王妍琪), Chuan-Zhao Zhang(张传钊), Jin-Quan Zhang(张金权), Song Li(李松), Meng Ju(巨濛), Wei-Guo Sun(孙伟国), Xi-Long Dou(豆喜龙), and Yuan-Yuan Jin(金园园)

Chin. Phys. B, 2023, 32 (**9**): 097402. DOI: 10.1088/1674-1056/acc934

Phonon-mediated superconductivity in orthorhombic XS (X = Nb, Ta or W)

Guo-Hua Liu(刘国华)[1], Kai-Yue Jiang(江恺悦)[1], Yi Wan(万一)[1], Shu-Xiang Qiao(乔树祥)[1], Jin-Han Tan(谭锦函)[1], Na Jiao(焦娜)[1], Ping Zhang(张平)[1,2], and Hong-Yan Lu(路洪艳)[1,†]

[1] *School of Physics and Physical Engineering, Qufu Normal University, Qufu* 273165, *China*
[2] *Institute of Applied Physics and Computational Mathematics, Beijing* 100088, *China*

(Received 18 September 2024; revised manuscript received 1 November 2024; accepted manuscript online 26 November 2024)

The unique three-dimensional orthorhombic NbS (o-NbS) compound synthesized in 1969 has recently been experimentally confirmed to be a superconductor [*Phys. Rev. B* **108** 174517 (2023)]. However, there is currently no theoretical research on its superconducting mechanism. In this work, we investigate the superconducting properties of o-NbS from first-principles calculations. Based on the Eliashberg equation, it is found that the superconductivity mainly originates from the coupling between the electrons of Nb-4d orbitals and the vibrations of Nb atoms in the low-frequency region and those of S atoms in the high-frequency region. A superconducting transition temperature (T_c) of 10.7 K is obtained, which is close to the experimental value and higher than most transition metal chalcogenides (TMCs). The calculated thermodynamic properties in the superconducting state, such as specific heat, energy gap, isotope coefficient, etc., also indicate that o-NbS is a conventional phonon-mediated superconductor. These results are consistent with recent experimental reports and provide a good understanding of the superconducting mechanism of o-NbS. Furthermore, the TMCs of o-TaS and o-WS are also investigated; these belong to the same and neighboring groups of Nb, and we find that o-TaS and o-WS are also phonon-mediated superconductors with T_c of 8.9 K and 7.2 K, respectively.

Keywords: first-principles calculations, phonon-mediated superconductivity, orthorhombic transition metal chalcogenides

PACS: 74.25.–q, 63.20.dk, 74.25.Jb, 74.20.Fg

DOI: 10.1088/1674-1056/ad9733 **CSTR:** 32038.14.CPB.ad9733

1. Introduction

Transition metal chalcogenides (TMCs) are generally composed of transition metal elements and sulfur group elements (such as sulfur, selenium, and tellurium).[1–3] Some of these TMCs are superconductors, which have been proven to be ideal materials for studying novel physical properties in the superconducting state, for example, the existence of electron–phonon-driven charge density waves, Ising pairing, orbital-selective multigap superconductivity and topological surface states.[4–15] Thus, it is of great theoretical significance to find superconductors among the TMCs.

As TMCs, NbS compounds have attracted extensive research. The first hexagonal lattice NbS (h-NbS) with NiAs type structure was prepared in 1954.[16–18] It has been experimentally reported that the h-NbS phase can be transformed into the o-NbS phase at a high temperature of 1053 K.[19] The o-NbS possesses a unique three-dimensional (3D) structure with Nb and S atoms in a distorted octahedral coordination environment.[20–22] It is of special interest to study the superconducting properties of o-NbS. It is known that one-dimensional (1D) and two-dimensional (2D) superconductivity has been found in TMCs, for example 1D Nb_3S_4 and 2D 2H-NbS_2.[20–22] Unlike 1D and 2D NbS compounds, o-NbS is a 3D structure and has a relatively simple structure among known NbS compounds. Therefore, o-NbS provides a good platform for theoretical research on the interplay between dimensionality, stoichiometry and superconductivity in Nb chalcogenide superconductors.

Recently, o-NbS was synthesized by solid-state reaction and the superconductivity of o-NbS with T_c of 6.0 K was experimentally confirmed by electrical, magnetic and heat transport measurements.[23,24] The coupling strength and normalized electronic specific heat analysis suggest that o-NbS is a fully gapped s-wave Bardeen–Cooper–Schrieffer (BCS) superconductor fitting perfectly with BCS theory. In addition, first-principles calculations have revealed the dominant role of the Nb-4d states. However, much more theoretical research on o-NbS is needed. Inspired by these works, it is of great significance to fully explore the superconducting mechanism of o-NbS from first-principles calculations.

In this paper, we prove the compound's dynamical stability and show that Nb and S atoms form ionic bonds. We also find that superconductivity mainly originates from the coupling between the electrons of Nb-4d orbitals and the vibrations of Nb atoms in the low-frequency region and those of S atoms in the high-frequency region. A T_c of 10.7 K is obtained, which is higher than that of most TMCs and is basically

†Corresponding author. E-mail: hylu@qfnu.edu.cn

© 2025 Chinese Physical Society and IOP Publishing Ltd. All rights, including for text and data mining, AI training, and similar technologies, are reserved.

in accordance with the reported experimental results. The calculated thermodynamic properties also indicate that o-NbS is a conventional phonon-mediated superconductor. The theoretical research into o-NbS gives a better understanding of the superconductivity of TMCs and provides a good explanation for recently reported experimental results.[24] In addition, similar methods are used to explore the TMCs of Ta and W, which belong to the same and adjacent groups as Nb. It is found that o-XS (X = Ta or W) are both conventional phonon-mediated superconductors. This work provides valuable insights into the broader family of TMCs.

2. Computational methods

This study employs density-functional theory (DFT) first-principles electronic calculations with the Vienna *ab initio* simulation package (VASP) code and the Quantum Espresso (QE) package.[25,26] The generalized gradient approximation (GGA) is applied to describe the exchange–correlation potentials with Perdew–Burke–Ernzerhof (PBE) parameterization.[27] With an energy cutoff of 600 eV, the lattice relaxation, charge density difference analysis, electronic band structure and electronic density of state (DOS) are calculated with the VASP package. The convergence parameters for energy and forces are taken to be 10^{-7} eV and 0.01 eV·Å^{-1}, respectively. A k-point grid of $6 \times 12 \times 6$ is chosen to calculate the relaxation, charge density difference analysis and electronic band structure. The electronic DOS is calculated with an $18 \times 36 \times 18$ k-point grid. Using the QE package, the phonon spectrum and electron–phonon coupling (EPC) in a $3 \times 6 \times 3$ q-point grid are utilized. The cutoff energies of the electron wave function and electron density are selected to be 80 Ry and 800 Ry, respectively. The EPC characteristics and superconductivity are calculated based on the Eliashberg equation, and the calculation formulae are detailed in the supplementary material.

3. Results and discussion

3.1. Crystal structure of o-NbS

After sufficient structural optimization, the fully relaxed lattice structure of o-NbS is shown in Fig. 1, where the green balls represent Nb atoms and the yellow balls represent S atoms. The lattice parameters are $a = 6.56$ Å, $b = 3.34$ Å, and $c = 5.78$ Å, which are in good accordance with experimental data ($a = 6.45$ Å, $b = 3.32$ Å and $c = 5.86$ Å).[24] In Fig. 1(a), each unit cell consists of four Nb atoms and four S atoms. There are four types of Nb–S bonds with lengths of 2.49 Å, 2.53 Å, 2.55 Å and 2.59 Å, respectively.

The charge density difference is shown in Fig. 1(b), and the electron localization function is represented in Figs. 1(c) and 1(d). The results for charge density difference show that the electrons transfer from the Nb atom to the S atom, and the further Bader charge analysis also demonstrates that each Nb atom loses 1.2e to the S atoms (Table 1). As a result, an ionic bond forms between each Nb atom and nearby S atoms. In fact, the presence of strong electron localization regions around the Nb and S atoms serves as evidence for the ionic bonding of the Nb atoms with S atoms, as shown in Figs. 1(c) and 1(d).

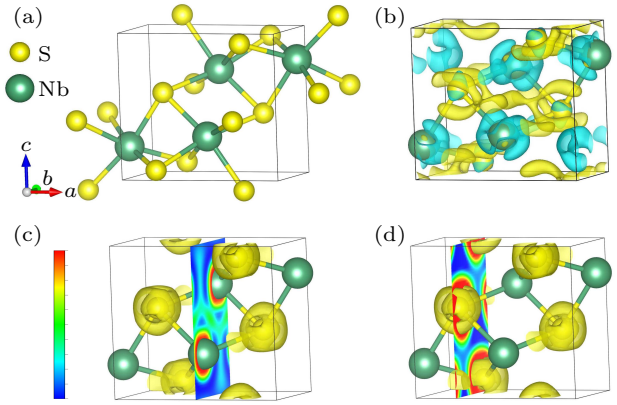


Fig. 1. (a) Crystal structure of o-NbS. (b) Charge density difference of o-NbS with cyan and yellow representing the loss and gain of electrons. 2D maps of the electron localization function for Nb (c) and S (d) of o-NbS.

Table 1. Bader charge (in units of $|e|$) for each atom in the o-NbS unit cell.

Atom	Nb_1	Nb_2	Nb_3	Nb_4	S_1	S_2	S_3	S_4
Charge	11.8	11.8	11.8	11.8	7.2	7.2	7.2	7.2

3.2. Electronic structure of o-NbS

The electronic band structure along high-symmetry lines and the DOS near the Fermi level were calculated. The spin–orbit coupling (SOC) effects on the energy band and DOS are considered in Figs. S1(a) and (b) in the supplementary material. In Fig. S1 we can see the effect of SOC on the energy band and the DOS is very small. The Fermi surface of the four energy bands passing through the Fermi level in Fig. S2(a) is in accordance with results in Fig. S1 as a higher Fermi velocity in Fig. S2 corresponds to a steeper energy band in Fig. S1. From Fig. S1 we also see that there is no significant band shift or splitting near the Fermi level, and the band structure remains basically unchanged. This implies that the effect of SOC can be neglected in describing the superconducting properties. Therefore, we carry out all calculations without SOC in the following.

The orbital-projected band structure of o-NbS is represented in Figs. 2(a) and 2(b). There are bands crossing the Fermi level, indicating that the material is metallic. From the orbital-projected band structure it can be seen that near the Fermi level the contribution mainly comes from the Nb-d_{z^2} orbital, and the lower one mainly originates from the d_{xz}, d_{xy} and $d_{x^2-y^2}$ orbitals of Nb atoms, while the contribution of S atoms is very small.

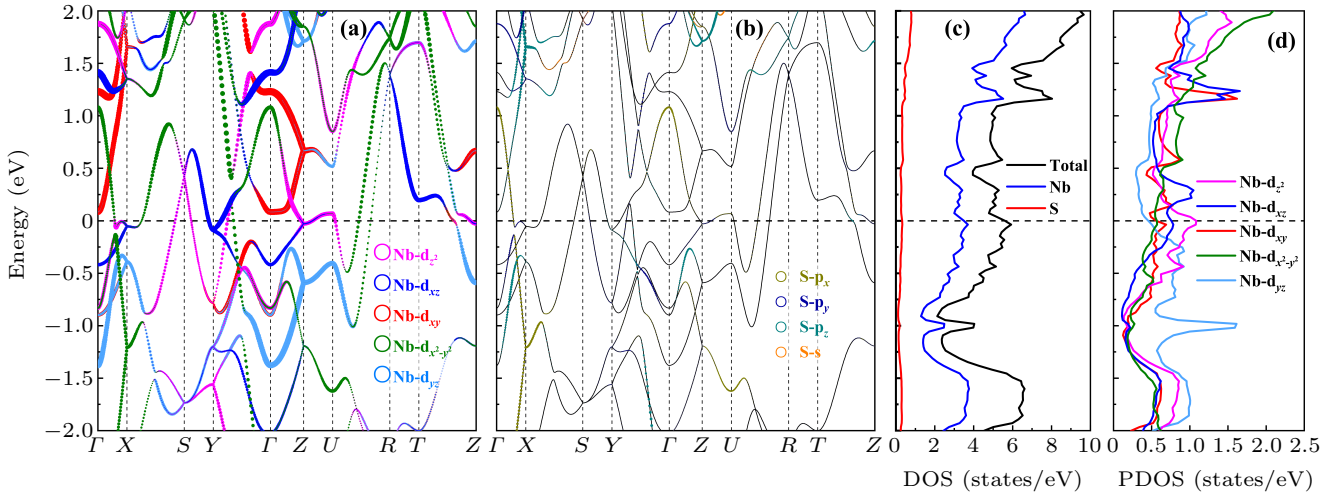


Fig. 2. [(a) and (b)] Orbital-projected electronic band structures of o-NbS along the high-symmetry line. (c) Total DOS and the DOS of Nb and S. (d) Projected density of states of o-NbS.

The DOS and projected density of states (PDOS) are shown in Figs. 2(c) and 2(d). In Fig. 2(c), the total DOS near the Fermi level is high, with a value of 5.6 states·eV^{-1} mainly due to the contribution of Nb atoms. The large total DOS near the Fermi level may be beneficial for a large EPC constant and lead to a high critical temperature of superconductivity. From Fig. 2(d) it can be seen that the largest contribution to the DOS near the Fermi level is from the Nb-d$_{z^2}$ orbital followed by the d$_{xz}$, d$_{xy}$ and d$_{x^2-y^2}$ orbitals of Nb atoms; the Nb-d$_{yz}$ orbital makes the smallest contribution. These results are highly consistent with the contribution of the orbital-projected band.

3.3. Electron–phonon coupling and superconductivity of o-NbS

The phonon spectrum of o-NbS was calculated and is shown in Fig. 3(a). The phonon spectrum is weighted by the magnitude λ_{qv} using different colors. The absence of an imaginary frequency in the phonon spectrum indicates that this material is dynamically stable. There are four Nb atoms and four S atoms in each unit cell, corresponding to three acoustic

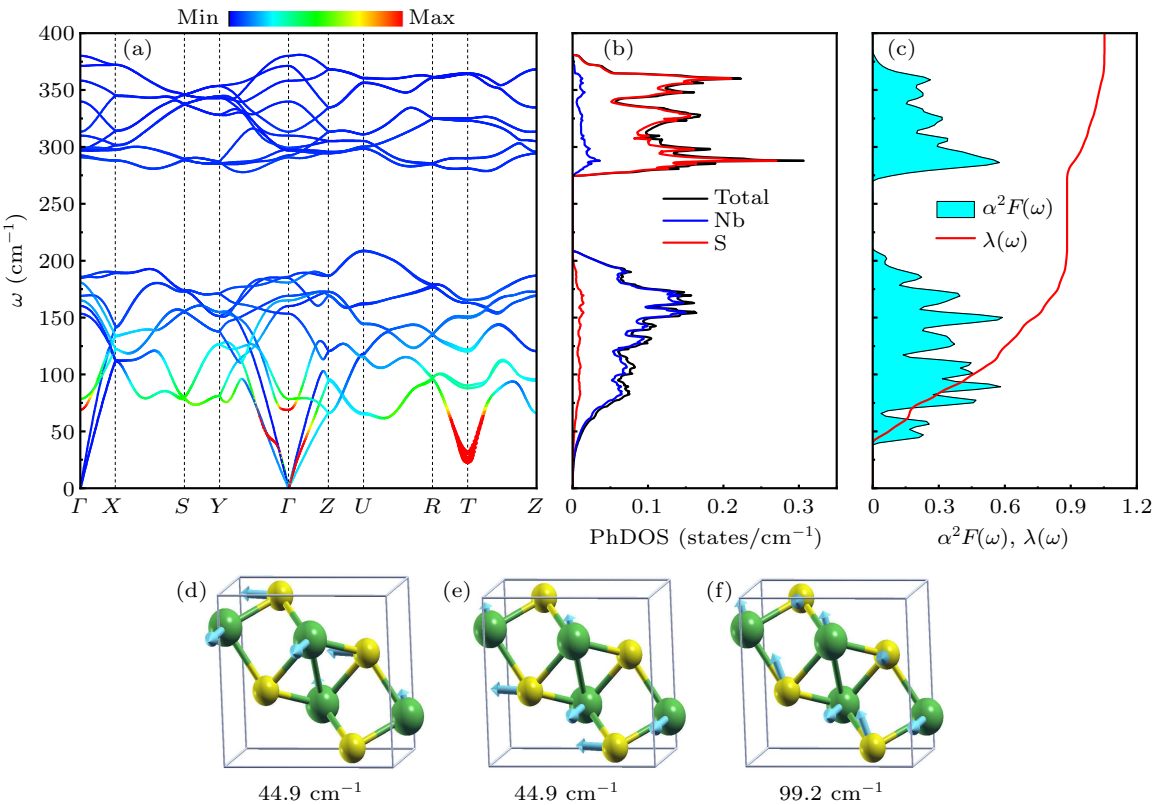


Fig. 3. (a) Phonon dispersions weighted by the magnitude of EPC λ_{qv}. (b) Total and atom-projected phonon DOS. (c) Elishberg spectral function $\alpha^2F(\omega)$ and the cumulative frequency dependence of EPC $\lambda(\omega)$. Panels (d)–(e) are vibration modes of o-NbS near the T point. The vibration frequencies are shown below each diagram. The green and yellow spheres represent Nb and S atoms, respectively. The arrows show the direction of the atomic vibration.

modes and 21 optical modes. In Figs. 3 and S3, 1–24 correspond to the atomic vibration pattern near the high-symmetry line T, where Nb atoms vibrate strongly in modes 1–12 and S atoms vibrate strongly in modes 13–24. Phonon modes 1–3 at the T points mainly contribute to strong electron–phonon interaction. In fact, there are 12 doubly degenerate phonon modes among those modes. Diagrams 1–3 show that the stretching vibration of Nb and S atoms in the vertical direction leads to the softening of phonon spectra. This mode exhibits strong interactions with electrons in Nb-4d orbitals, which is beneficial for improving T_c.

In Fig. 3(a), the low-frequency phonons at T show a significant downward trend, and the low-frequency phonons interact strongly with electrons, which may account for the emergence of superconductivity with high T_c. The phonon density of states (PhDOS), Elishberg spectral function $\alpha^2F(\omega)$ and accumulative EPC are also calculated, as shown in Figs. 3(b) and 3(c). The decomposition of phonon spectra provides more information about the vibrations of atoms. As can be seen from Fig. 3(b), in the frequency region below 200 cm^{-1}, the main contribution to the total EPC $\lambda(\omega)$ comes from the vibrations of Nb atoms, while above 275 cm^{-1} it comes from the vibrations of S atoms, which is in accordance with the fact that Nb atoms vibrate strongly in the low-frequency region and S atoms vibrate strongly in high-frequency region, as shown in 1–3 in Fig. 3 and 4–24 in Fig. S3. In Fig. 3(c), the low-frequency phonons in the range of 0–200 cm^{-1} contribute almost 84% of the total λ and the optical branches in the frequency above 275 cm^{-1} contribute almost 16% of the total λ. This is natural since S atoms are lighter than Nb atoms. A large EPC together with a high critical superconducting temperature is expected due to the high electronic DOS at the Fermi level. The calculations show that the total EPC constant λ is 1.05 and the corresponding T_c is 10.7 K.

It is well known that T_c is usually related to the Coulomb pseudopotential μ^*. T_c with respect to μ^* is shown in Fig. S4. We choose series values of μ^* in the range of 0.05–0.15: T_c decreases with increasing μ^*, which is similar to the case in Ref. [33]. As μ^* increases from 0.05 to 0.15, the T_c of o-NbS decreases from 15.5 K to 9.9 K. In this work, we choose $\mu^* = 0.13$ in accordance with the experimental values.[24]

3.4. Electron–phonon coupling and superconductivity of o-XS (X = Ta or W)

Additionally, we study the superconductivity of o-XS (X = Ta or W). The orbital-projected bands of o-XS are shown in Figs. S5(a), S5(b), S6(a), and S6(b). The materials are metallic as there are bands crossing the Fermi level. The DOS and PDOS are shown in Fig. S5(c), S5(d), S6(c), and S6(d). It can be seen that near the Fermi level, the electronic DOS mainly originates from Ta or W-4d orbitals and the contribution of S atoms is small, which is similar to the case of NbS.

The phonon spectra of o-XS are calculated and shown in Figs. S7(a) and S8(a). The o-XS are stable as there is no imaginary frequency in the phonon spectrum. The PhDOS, Elishberg spectral function $\alpha^2F(\omega)$ and accumulative EPC are shown in Figs. S7(b), S7(c), S8(b), and S8(c). In the low-frequency region, the main contribution to the total EPC $\lambda(\omega)$ comes from the vibrations of Ta or W atoms, while in the high-frequency region, it mainly comes from the vibrations of S atoms, which is the same as behavior of NbS. In all, we find that superconducting properties of o-XS are similar to those of o-NbS. The theoretically obtained T_c of o-TaS and o-WS are 8.9 K and 7.2 K, respectively, which are smaller than the T_c (10.7 K) of o-NbS. The corresponding superconducting properties are shown in Table 2.

Table 2. Superconducting T_c (K), total EPC constant λ, logarithmically averaged phonon frequency ω_{log} (K), DOS at the Fermi level $N(E_F)$ (states/spin/Ry/unit cell), Sommerfeld constant γ (mJ·cm^{-3}·K^{-2}), specific heat jump at T_c $\Delta C(T_c)$ (mJ·cm^{-3}·K^{-2}), superconducting gap at 0 K $\Delta(0)$ (meV), critical magnetic field at 0 K $H_c(0)$ (T), isotope coefficient α, and $2\Delta(0)/k_BT_c$ for o-XS (X = Nb, Ta or W).

Compound	T_c	λ	ω_{log}	$N(E_F)$	γ	$\Delta C(T_c)$	$\Delta(0)$	$H_c(0)$	α	$2\Delta(0)/k_BT_c$
NbS	10.7	1.03	168.86	33.22	0.31	0.59	1.79	0.15	0.46	3.89
TaS	8.9	1.05	135.96	30.26	0.29	0.56	1.49	0.12	0.46	3.91
WS	7.2	0.84	169.92	29.64	0.27	0.46	1.16	0.09	0.44	3.73

3.5. Thermodynamic properties of o-XS (X = Nb, Ta or W)

Finally, the thermodynamic properties such as critical magnetic field $H_c(0)$, superconducting gap $\Delta(0)$, specific heat jump $\Delta C(T_c)$ and isotope coefficient α of XS (X = Nb, Ta or W) were calculated by the following semiempirical formulae:[32]

$$\frac{\gamma T_c^2}{H_c^2(0)} = 0.168\left[1 - 12.2\left(\frac{T_c}{\omega_{log}}\right)^2 \ln\left(\frac{\omega_{log}}{3T_c}\right)\right], \quad (1)$$

$$\frac{2\Delta(0)}{k_BT_c} = 3.53\left[1 + 12.5\left(\frac{T_c}{\omega_{log}}\right)^2 \ln\left(\frac{\omega_{log}}{2T_c}\right)\right], \quad (2)$$

$$\frac{\Delta C(T_c)}{\gamma T_c} = 1.43\left[1 + 53\left(\frac{T_c}{\omega_{log}}\right)^2 \ln\left(\frac{\omega_{log}}{3T_c}\right)\right], \quad (3)$$

$$\alpha = \frac{1}{2}\left[1 - \frac{1.04(1+\lambda)(1+0.62\lambda)}{[\lambda - \mu^*(1+0.62\lambda)]^2}\mu^{*2}\right], \quad (4)$$

$$\gamma = \frac{2}{3}\pi^2 k_B^2 N(E_F)(1+\lambda). \quad (5)$$

Here k_B is the Boltzmann constant.

The calculated results are shown in Table 2. It is worth noting that the calculated values of $\frac{2\Delta(0)}{k_B T_c}$ and α for o-NbS are 3.89 and 0.46, respectively, which are close to those obtained from conventional BCS theoretical calculations ($\frac{2\Delta(0)}{k_B T_c} \approx 3.53$ and $\alpha \approx 0.5$), suggesting that the materials are conventional phonon-mediated superconductors. Besides, the calculated total EPC constant (λ) of 1.05 and T_c of 10.7 K are comparable to the experimental values for λ of 0.59 and T_c of 6.0 K. We carried out more calculations and found that these materials have no magnetism, charge order wave or other possible orders, which also support the phonon-mediated superconductivity in o-NbS, o-TaS and o-WS.

4. Conclusion

In summary, we have investigated the superconductivity of o-NbS from first principles. We found that the superconductivity mainly originates from coupling between the electrons of Nb-4d orbitals and the vibrations of Nb atoms in the low-frequency region and those of S atoms in the high-frequency region. In addition, the TMCs of o-TaS and o-WS were also investigated. We found that o-XS (X = Ta or W) are phonon-mediated superconductors with T_cs of 8.9 K and 7.2 K, respectively. We carried out more calculations and found that these materials have no magnetism, charge order wave or other possible orders, also supporting the phonon-mediated superconductivity in o-NbS, o-TaS and o-WS. Thus, this research provides more understanding of the superconducting mechanism of TMCs.

Acknowledgments

Project supported by the National Natural Science Foundation of China (Grant Nos. 12074213 and 11574108), the Major Basic Program of Natural Science Foundation of Shandong Province (Grant No. ZR2021ZD01), the Natural Science Foundation of Shandong Province (Grant No. ZR2023MA082), and the Project of Introduction and Cultivation for Young Innovative Talentsin Colleges and Universities of Shandong Province.

References

[1] Coleman J N, Lotya M, ONeill A, *et al.* 2011 *Science* **331** 568
[2] Lotsch B V 2015 *Annu. Rev. Mater. Res.* **45** 85
[3] Ryu H, Chen Y, Kim Heejung, *et al.* 2018 *Nano Lett.* **18** 689
[4] Valla T, Fedorov A V, Johnson P D, Glans P A, McGuinness C, Smith K E, Andrei E Y and Berger H 2004 *Phys. Rev. Lett.* **92** 086401
[5] Weber F, Rosenkranz S, Castellan J P, Osborn R, Hott R, Heid R, Bohnen K P, Egami T, Said A H and Reznik D 2011 *Phys. Rev. Lett.* **107** 107403
[6] Malliakas C D and Kanatzidis M G 2013 *J. Am. Chem. Soc.* **135** 1719
[7] Xi X, Wang Z, Zhao W, Park J H, Law K T, Berger H, Forró L, Shan J and Mak K F 2016 *Nat. Phys.* **12** 139
[8] Zhang H, Rousuli A, Zhang K, *et al.* 2022 *Nat. Phys.* **18** 1425
[9] Yokoya T, Kiss T, Chainani A, Shin S, Nohara M and Takagi H 2001 *Science* **294** 2518
[10] Bi X, Li Z, Huang J, *et al.* 2022 *Phys. Rev. Res.* **4** 013188
[11] Xu J P, Wang M X, Liu Z L, *et al.* 2015 *Phys. Rev. Lett.* **114** 017001
[12] Van Maaren M and Schaeffer G 1966 *Phys. Lett.* **20** 131
[13] Witteveen C, Górnicka K, Chang J, Mnsson M, Klimczuk T and Von Rohr F O 2021 *Dalton Trans.* **50** 3216
[14] Devarakonda A, Inoue H, Fang S, Ozsoy-Keskinbora C, Suzuki T, Kriener M, Fu L, Kaxiras E, Bell D C and Checkelsky J G 2020 *Science* **370** 231
[15] Kckerling M, Johrendt D and Finckh E W 1998 *J. Am. Chem. Soc.* **120** 12297
[16] Blitz W and Köcher A 1938 *Z. Anorg. Allg. Chem.* **237** 369
[17] Schönberg N 1954 *Acta Metall.* **2** 427
[18] An Y, Chen J, Yan Y, Wang J, Zhou Y, Wang Z, Ma C, Wang T, Wu R and Liu W 2023 *Phys. Rev. B* **108** 054519
[19] Kadijk F and Jellinek F J 1969 *Less-Common Met.* **19** 421
[20] Amberger E, Polborn K, Grimm P, Dietrich M and Obst B 1978 *Solid State Commun.* **26** 943
[21] Jellinek F, Brauer G and Mller H 1960 *Nature* **185** 376
[22] Rijnsdorp J and Jellinek F 1978 *J. Solid State Chem.* **25** 325
[23] Narayan P B V and Finnemore D K 1978 *J. Less-Common Met.* **61** 231
[24] Ruan B B, Yi J K, Chen L W, Zhou M H, Shi Y Q, Yang Q S, Gu Y D, Chen G F and Ren Z A 2023 *Phys. Rev. B* **108** 174517
[25] Kresse G and Furthmüller J 1996 *Phys. Rev. B* **54** 11169
[26] Giannozzi P, Baroni S, Bonini N, *et al.* 2009 *J. Phys.: Condens. Matter.* **21** 395502
[27] Perdew J P, Burke K and Ernzerhof M 1996 *Phys. Rev. Lett.* **77** 3865
[28] McMillan W L 1968 *Phys. Rev.* **167** 331
[29] Dynes R C 1972 *Solid State Commun.* **10** 615
[30] Allen P B and Dynes R C 1975 *Phys. Rev. B* **12** 905
[31] Giustino F 2017 *Rev. Mod. Phys.* **89** 015003
[32] Carbotte J P 1990 *Rev. Mod. Phys.* **4** 62
[33] Jiao N, Liu H D, Yang L, Li Y P, Zheng M M, Lu H Y and Zhang P 2022 *Europhys. Lett.* **138** 46002
[34] Sarkar S and Das A N 1994 *Phys. Rev. B* **49** 13070